ÉCOLE POLYTECHNIQUE
FÉDÉRALE DE LAUSANNE

MATHICSE
Mathematics Institute of Computational Science and Engineering
School of Basic Sciences - Section of Mathematics

MATHICSE Technical Report
Nr. 43.2013
December 2013

Stabilized reduced basis method for parametrized advection-diffusion PDEs

P. Pacciarini, G. Rozza

http://mathicse.epfl.ch

Phone: +41 21 69 37648

Address:
EPFL - SB - MATHICSE (Bâtiment MA)
Station 8 - CH-1015 - Lausanne - Switzerland

Fax: +41 21 69 32545

Stabilized reduced basis method for parametrized advection-diffusion PDEs

Paolo Pacciarini[a], Gianluigi Rozza[b,c,*]

[a] *MOX - Modellistica e Calcolo Scientifico, Dipartimento di Matematica F. Brioschi, Politecnico di Milano, P.za Leonardo da Vinci 32, I-20133, Milano, Italy*

[b] *now at SISSA mathLab, International School for Advanced Studies, Via Bonomea 265, I-34136 Trieste, Italy*

[c] *CMCS - Modelling and Scientific Computing, MATHICSE - Mathematics Institute of Computational Science and Engineering, EPFL - Ecole Polytechnique Fédérale de Lausanne, Station 8, CH-1015 Lausanne, Switzerland*

Abstract

In this work, we propose viable and efficient strategies for the stabilization of the reduced basis approximation of an advection dominated problem. In particular, we investigate the combination of a classic stabilization method (SUPG) with the Offline-Online structure of the RB method. We explain why the stabilization is needed in both stages and we identify, analytically and numerically, which are the drawbacks of a stabilization performed only during the construction of the reduced basis (i.e. only in the Offline stage). We carry out numerical tests to assess the performances of the "double" stabilization both in steady and unsteady problems, also related to heat transfer phenomena.

Keywords: reduced basis, advection dominated problems, stabilization methods.

1. Introduction

The aim of this work is to study and develop a *stabilized reduced basis method* suitable for the approximation of the solution of parametrized advection-diffusion PDEs with high Péclet number, that is, roughly, the ratio between the advection term and the diffusion one.

Advection-diffusion equations are very important in many engineering applications, because they are used to model, for example, heat transfer phenomena (with conduction and convection) [16] or the diffusion of pollutants in the atmosphere or in the water [6, 26]. In such applications, we often need very fast evaluations of the approximated solution, depending on some physical and/or geometrical input parameters. This happens, for example, in the case of *real-time* simulations. Moreover, we need rapid evaluations also if we have to perform repeated approximation of the solution, for different input parameters. An important case of this *many-query* situation is represented by some optimization problems, in which the objective function to optimize depends on the parameters through the solution of a PDE.

The reduced basis (RB) method [25, 29] meets our need for rapidity and it is also able to guarantee the *reliability* of the solution, thanks to sharp *a posteriori* error bounds. A crucial feature of the RB method is its decomposition into two computational steps. During the first expensive one, called *Offline* step, some high-fidelity approximated solutions are computed, which will become the global basis functions of the Galerkin projections performed during the second inexpensive phase, called *Online* step. A brief introduction to the RB method will be given in Section 2.

*Corresponding author

Email addresses: paolo.pacciarini@polimi.it (Paolo Pacciarini), grozza@sissa.it (Gianluigi Rozza)

As the advection-diffusion equations are often used to model heat transfer phenomena, we can find in literature many results about the RB approximation of heat transfer problems such as the Poiseuille-Graetz problem or the "thermal fin" problem [9, 20, 25, 28, 30, 31]. However, until now, only the case in which the Péclet number is reasonably low (i.e. $\sim 10^2$) was considered without stabilization.

When the Péclet number is higher (i.e. $\sim 10^5$), it is very well known [27] that the Finite Element (FE) solution of the advection-diffusion equation - that the RB method aims to recover - can show significant instability phenomena. In order to fix this problem, in the RB framework, some solutions have been proposed for the steady case [6, 7, 24, 26]. The basic idea is to consider as *truth* solution a stabilized FE one, using some classical stabilization method (e.g. the SUPG method [27]), and then to perform the RB *Offline* and *Online* steps using the stabilized bilinear form instead of the original one. In the cited papers we can find some applications to environmental sciences and engineering problems concerning, in particular, air pollution. Very recently, also a Petrov-Galerkin based strategy has been proposed to deal with high Péclet number problems [5].

In some of the previous works, the issue of stability was not studied too much inside concerning the Offline-Online affine decomposition and some proposed options were not very viable for more complex problems [26]. Our aim was not only to increase the Péclet number in parametrized problems dealing with convection and transport, including parametrized moving inner fronts and boundary layers. This work has been also motivated by the aim of creating a general stabilized framework to provide some explanations of previous approaches and known results in literature.

In our work we then want to go further in the study of the *stabilized RB method*, proposing viable and efficient strategies to be used combined with the Offline-Online computational procedures and providing a deeper analysis on the need of stabilization for parametrized advection-diffusion problems. We start by studying steady problems and then we move to the time dependent case.

After having done, in Section 2, a short presentation of the RB method, in Section 3 we observe and analyse what happens when we "stabilize" only the Offline stage of the RB method, thus producing "stable" basis functions to be interpolated in the Online stage by projecting with respect to the non-stabilized advection-diffusion operator. We will show that, in general, the latter strategy is not satisfactory because of "inconsistency" problems between the Offline and Online stages, arising from the use of two different bilinear forms. We will also prove an *a priori* error estimate (Proposition 3.1) in order to estimate this inconsistency. After having determined which stabilization strategy gives better results and why, in Section 4 we will try to apply it to a test problem with a parameter dependent internal layer, using also a piecewise quadratic polynomial *truth* approximation space. Finally, in Section 5 we extend the investigation of the RB stabilization method to parabolic problems.

2. A brief review of the reduced basis method

The reduced basis (RB) method is a reduced order modelling (ROM) technique which provides rapid and reliable solutions for parametrized partial differential equations (PPDEs), in which the parameters can be either physical or geometrical [25, 29].

The need to solve this kind of problems arises in many engineering applications, in which the evaluation of some *output* quantities is required. These *outputs* are often function of the solution of a PDE, which can in turn depend on some *input* parameters. The aim of the RB method is to provide a very fast computation of this *input-output* evaluation.

Roughly speaking, given a value of the parameter, the (Lagrange) RB method consists in a Galerkin projection of the continuous solution on a particular subspace of a high-fidelity approximation space, e.g. a finite element (FE) space with a large number of degrees of freedom. This subspace is the one spanned by some pre-computed high-fidelity global solutions (*snapshots*) of the continuous parametrized problem, corresponding to some properly chosen values of the parameter.

For a complete presentation of the reduced basis method we refer to [25, 29], now we just recall its main features and we introduce some notations.

2.1. The continuous problem

Let $\boldsymbol{\mu}$ belong to the *parameter domain* $\mathcal{D}$, a subset of $\mathbb{R}^P$. Let Ω be a regular bounded open subset of $\mathbb{R}^d$ ($d = 1, 2, 3$) and X a suitable Hilbert space. Given a parameter value $\boldsymbol{\mu} \in \mathcal{D}$, let $a(\cdot, \cdot; \boldsymbol{\mu})\colon X \times X \to \mathbb{R}$ be a bilinear form and let $F(\cdot; \boldsymbol{\mu})\colon X \to \mathbb{R}$ be a linear functional. As we will focus on advection-diffusion equations, that are second order elliptic PDE, the space X will be such that $H_0^1(\Omega) \subset X \subset H^1(\Omega)$. Formally, our problem can be written as follows:

$$\begin{aligned} &\text{find } u(\boldsymbol{\mu}) \in X \text{ s.t.} \\ &a(u(\boldsymbol{\mu}), v; \boldsymbol{\mu}) = F(v; \boldsymbol{\mu}) \quad \forall v \in X. \end{aligned} \tag{1}$$

The coercivity and continuity assumption on the form a can now be expressed by, respectively:

$$\exists\, \alpha_0 > 0 \quad \text{s.t.} \quad \alpha_0 \leq \alpha(\boldsymbol{\mu}) = \inf_{v \in X} \frac{a(v, v; \boldsymbol{\mu})}{\|v\|_X^2} \quad \forall \boldsymbol{\mu} \in \mathcal{D} \tag{2}$$

and

$$+\infty > \gamma(\boldsymbol{\mu}) = \sup_{v \in X} \sup_{w \in X} \frac{|a(v, w; \boldsymbol{\mu})|}{\|v\|_X \|w\|_X} \quad \forall \boldsymbol{\mu} \in \mathcal{D}. \tag{3}$$

We shall make now an important assumption: the *affine* dependency of a on the parameter $\boldsymbol{\mu}$. With *affine*, we mean that the form can be written in the following way:

$$a(v, w; \boldsymbol{\mu}) = \sum_{q=1}^{Q_a} \Theta_a^q(\boldsymbol{\mu}) a^q(v, w) \quad \forall \boldsymbol{\mu} \in \mathcal{D}. \tag{4}$$

Here, $\Theta_a^q\colon \mathcal{D} \to \mathbb{R}$, $q = 1, \ldots, Q_a$, are smooth functions, while $a^q\colon X \times X \to \mathbb{R}$, $q = 1, \ldots, Q_a$, are $\boldsymbol{\mu}$-independent continuous bilinear forms. This assumption turns out to be crucial for performing the Offline-Online decoupling of the computation [25, 29]. At last we assume that also the functional F depends "affinely" on the parameter:

$$F(v; \boldsymbol{\mu}) = \sum_{q=1}^{Q_F} \Theta_F^q(\boldsymbol{\mu}) F^q(v) \quad \forall \boldsymbol{\mu} \in \mathcal{D}, \tag{5}$$

where, also in this case, $\Theta_F^q\colon \mathcal{D} \to \mathbb{R}$, $q = 1, \ldots, Q_F$, are smooth functions, while $F^q\colon X \to \mathbb{R}$, $q = 1, \ldots, Q_a$, are continuous linear functionals.

We assume that $X^{\mathcal{N}}$ is a conforming finite element space with $\mathcal{N}$ degrees of freedom, we can now set the *truth* approximation of the problem (1):

$$\begin{aligned} &\text{find } u^{\mathcal{N}}(\boldsymbol{\mu}) \in X^{\mathcal{N}} \text{ s.t.} \\ &a^{\mathcal{N}}(u^{\mathcal{N}}(\boldsymbol{\mu}), v^{\mathcal{N}}; \boldsymbol{\mu}) = F(v^{\mathcal{N}}; \boldsymbol{\mu}) \quad \forall v^{\mathcal{N}} \in X^{\mathcal{N}}. \end{aligned} \tag{6}$$

The bilinear forms involved in the truth approximation can be different from the continuous one, as in the SUPG stabilization case that we will introduce later. As regards the coercivity of $\alpha^{\mathcal{N}}$ we define

$$\alpha^{\mathcal{N}}(\boldsymbol{\mu}) := \inf_{v^{\mathcal{N}} \in X^{\mathcal{N}}} \frac{a^{\mathcal{N}}(v^{\mathcal{N}}, v^{\mathcal{N}}; \boldsymbol{\mu})}{\|v\|_X^2} \quad \forall \boldsymbol{\mu} \in \mathcal{D}. \tag{7}$$

Similarly, for the continuity, we can define

$$\gamma^{\mathcal{N}}(\boldsymbol{\mu}) := \sup_{v^{\mathcal{N}} \in X^{\mathcal{N}}} \sup_{w^{\mathcal{N}} \in X^{\mathcal{N}}} \frac{|a^{\mathcal{N}}(v^{\mathcal{N}}, w^{\mathcal{N}}; \boldsymbol{\mu})|}{\|v^{\mathcal{N}}\|_X \|w^{\mathcal{N}}\|_X} \quad \forall \boldsymbol{\mu} \in \mathcal{D}. \tag{8}$$

In the case that $a^{\mathcal{N}} = a$ we easily obtain, by restriction, that $\alpha(\boldsymbol{\mu}) \leq \alpha^{\mathcal{N}}(\boldsymbol{\mu})$ and $\gamma^{\mathcal{N}}(\boldsymbol{\mu}) \leq \gamma(\boldsymbol{\mu})$ for all $\boldsymbol{\mu} \in \mathcal{D}$.

As we have already mentioned, also the domain of the equation can depend on the parameter. In this case we need to map the parametric domain onto a reference one denoted with Ω, via a suitable parameter-dependent transformation $T(\cdot;\boldsymbol{\mu})\colon \Omega \to \Omega_o(\boldsymbol{\mu})$, see [25, 29], which allows to track back on the reference domain Ω all the bilinear and linear forms involved. The reference domain can be defined by choosing the original domain corresponding to a particular value of the parameter. In this work we used only affine mappings [25, 29] that allow to easily recover the affinity assumptions (4) and (5). In [25, 29] it is possible to find, in particular, a detailed treatment of the advection-diffusion operators.

2.2. The reduced basis method: main features

Let us suppose that we are given a problem in the form (1) and its *truth* approximation (6). We recall that the dimension of the finite element space $X^{\mathcal{N}}$ is $\mathcal{N}$. We introduce now a set of N suitably chosen parameter values, $S_N = \{\boldsymbol{\mu}^1, \ldots, \boldsymbol{\mu}^N\}$, and we can define the *reduced basis space*: $X_N^{\mathcal{N}} = \text{span}\{u^{\mathcal{N}}(\boldsymbol{\mu}^n) \,|\, 1 \leq n \leq N\}$. Actually, we do not consider this set of particular solution as a basis, but we perform a Gram-Schmidt orthonormalization process on it [25, 29].

Given a value $\boldsymbol{\mu} \in \mathcal{D}$ of the parameter we define the RB solution $u_N^{\mathcal{N}}(\boldsymbol{\mu})$ such that:

$$a^{\mathcal{N}}(u_N^{\mathcal{N}}(\boldsymbol{\mu}), v_N; \boldsymbol{\mu}) = F(v_N; \boldsymbol{\mu}) \quad \forall v_N \in X_N^{\mathcal{N}}. \tag{9}$$

Recalling that $N \ll \mathcal{N}$, we emphasize the fact that to find the RB solution we need just to solve a $N \times N$ linear system, instead of the $\mathcal{N} \times \mathcal{N}$ one of the FE method.

The set S_N is built in the Offline stage, together with the particular solutions which span $X_N^{\mathcal{N}}$, using a Greedy algorithm [25, 29]. The latter chooses, at each step, the parameter value which maximizes a suitable *a posteriori* error estimator $\boldsymbol{\mu} \mapsto \Delta_N(\boldsymbol{\mu})$ such that

$$|||u^{\mathcal{N}}(\boldsymbol{\mu}) - u_N^{\mathcal{N}}(\boldsymbol{\mu})|||_{\boldsymbol{\mu}} \leq \Delta_N(\boldsymbol{\mu}) \quad \forall \boldsymbol{\mu} \in \mathcal{D}^1 \tag{10}$$

and the algorithm stops when a prescribed tolerance ε_{tol}^* is reached, that is when $\Delta_N(\boldsymbol{\mu}) \leq \varepsilon_{tol}^*$ for each parameter value $\boldsymbol{\mu}$ in a training set $\Xi_{train} \subset \mathcal{D}$.

The error estimator has to be sharp, in order to avoid an unnecessarily high dimension N of the reduced basis space. Moreover, it must be computationally inexpensive in order to speed up the Greedy algorithm (within which it is computed many times) and to allow the certification of the RB solution during the Online stage. The estimator Δ_N is based on the residual and it requires the computation of a lower bound $\boldsymbol{\mu} \mapsto \alpha_{LB}(\boldsymbol{\mu})$ for the coercivity constant (2), which can be computed using the Successive Constraint Method (SCM) [15, 29].

We want to point out that all the expensive computations (i.e. those whose cost depend on the FE space dimension $\mathcal{N}$) are performed during the Offline stage.

As already mentioned before, the affinity assumptions (4) and (5) are crucial for the Offline-Online decoupling, as it is extensively shown in [25, 29]. If the latter assumptions are not fulfilled, it turns out to be necessary an interpolation strategy (e.g. empirical interpolation [1]) in order to recover them.

The affinity assumptions allow the storage, during the Offline stage, of the matrices corresponding to the parameter independent forms a_q, $q = 1, \ldots, Q_a$, restricted to $X_N^{\mathcal{N}}$. Thanks to this fact, during the Online stage the assembly of the reduced basis system only consists in a linear combination of these pre-computed matrices. A similar strategy can also be applied to the computation of the error estimator [25, 29].

[1] Here $|||\cdot|||_{\boldsymbol{\mu}}$ is the norm induced by the symmetric part of the bilinear form $a(\cdot,\cdot;\boldsymbol{\mu})$. See (28) for the definition.

3. Stabilized reduced basis: introduction and numerical tests

The main goal of this section is to design an efficient stabilization procedure for the RB method. More specifically, we will make a comparison between an *Offline-Online stabilized* method and an *Offline-only stabilized* one, when used to approximate the solution of a parametric advection-diffusion problem:

$$-\varepsilon(\boldsymbol{\mu})\Delta u(\boldsymbol{\mu}) + \boldsymbol{\beta}(\boldsymbol{\mu}) \cdot \nabla u(\boldsymbol{\mu}) = 0 \quad \text{on } \Omega. \tag{11}$$

given a parameter value $\boldsymbol{\mu} \in \mathcal{D}$ and suitable Dirichlet, Neumann or mixed boundary conditions. Here Ω is an open subset of $\mathbb{R}^2$, while $\varepsilon(\boldsymbol{\mu})$ and $\boldsymbol{\beta}(\boldsymbol{\mu})$ are functions $\Omega \to [0, +\infty)$ and $\Omega \to \mathbb{R}^2$, respectively.

It is well known from the general theory of the numerical approximation of advection-diffusion equations, that the FE solution of such equations can show significant instability phenomena when the advective term dominates the diffusive one. Let us try to give a more detailed explanation. Let $\mathcal{T}_h$ be a triangulation of Ω and let K be an element of $\mathcal{T}_h$. We say that a problem is *advection dominated in* K if the following condition holds:

$$\mathbb{P}\mathrm{e}_K(\boldsymbol{\mu})(x) := \frac{|\boldsymbol{\beta}(\boldsymbol{\mu})(x)|h_K}{2\varepsilon(\boldsymbol{\mu})(x)} > 1 \quad \forall \boldsymbol{x} \in K \quad \forall \boldsymbol{\mu} \in \mathcal{D}, \tag{12}$$

where h_K is the diameter of K. It is very well known from literature (e.g. [27]) the FE approximation of advection dominated problems can show significant instability phenomena, e.g. spurious oscillations near the boundary layers. Several ways have been proposed to fix these problems. We choose to resort to a strongly consistent stabilization method: the *Streamline/Upwind Petrov-Galerkin* (SUPG) [3, 13, 18, 19]. For a detailed presentation of the stabilization method for the FE approximation of advection dominated problems, we refer to [27].

Let us now explain the basic ideas of the two RB stabilization methods mentioned before. As regards the *Offline-Online stabilized* method, the choice of the name reveals that the Galerkin projections are performed, in both Offline and Online stage, with respect to the SUPG stabilized bilinear form that is

$$\begin{aligned} a_{stab}(w^{\mathcal{N}}, v^{\mathcal{N}}; \boldsymbol{\mu}) = &\int_\Omega \varepsilon(\boldsymbol{\mu}) \nabla w^{\mathcal{N}} \cdot \nabla v^{\mathcal{N}} + (\boldsymbol{\beta}(\boldsymbol{\mu}) \cdot \nabla w^{\mathcal{N}}) v^{\mathcal{N}} \\ &+ \sum_{K \in \mathcal{T}_h} \delta_K \int_K L^{\boldsymbol{\mu}} v^{\mathcal{N}} \left(\frac{h_K}{|\boldsymbol{\beta}(\boldsymbol{\mu})|} L^{\boldsymbol{\mu}}_{SS} v^{\mathcal{N}} \right) \end{aligned} \tag{13}$$

with $w^{\mathcal{N}}, v^{\mathcal{N}}$ chosen in a suitable piecewise polynomial space $X^{\mathcal{N}}$. In (13) $L^{\boldsymbol{\mu}}$ is the parameter dependent advection-diffusion operator, that is $L^{\boldsymbol{\mu}} v^{\mathcal{N}} = -\varepsilon(\boldsymbol{\mu})\Delta v^{\mathcal{N}} + \boldsymbol{\beta}(\boldsymbol{\mu}) \cdot \nabla v^{\mathcal{N}}$, which can be splitted in its symmetric part $L^{\boldsymbol{\mu}}_S$ and in its skew-symmetric one $L^{\boldsymbol{\mu}}_{SS}$ [27]. In the case of a divergence free advection field $\boldsymbol{\beta}$ (as in our numerical tests), we have

$$L^{\boldsymbol{\mu}}_S v^{\mathcal{N}} = -\varepsilon(\boldsymbol{\mu})\Delta v^{\mathcal{N}}, \quad L^{\boldsymbol{\mu}}_{SS} v = \boldsymbol{\beta}(\boldsymbol{\mu}) \cdot \nabla v^{\mathcal{N}}. \tag{14}$$

The bilinear form a_{stab} is coercive, so we can apply the already developed theory in order to use the reduced basis method.

We want then to understand the behaviour of the *Offline-only stabilized* method, which consists in using the stabilized form (13) only during the Offline stage and then projecting, during the Online stage, with respect to the standard advection-diffusion bilinear form. To motivate this choice, we recall that the RB approximation is actually a linear combination of particularly chosen *truth* solutions of the problem. Thus, if we consider stable *truth* approximations when building the reduced basis, it seems reasonable to expect RB approximations which does not show instability. Moreover, note that the *Offline-only* method is strongly consistent with respect to the continuous advection-diffusion problem.

The advantage of using the *Offline-only stabilized* method would be a certain reduction of the computational cost, that could be significant if the number of affine stabilization terms is very high.

We will start from the study of some quite simple test problems, for which it is straightforward to obtain the affine expansion. The first one, in Section 3.1, is a problem that shows strong instability effect that can be effectively fixed by the *Offline-Online stabilized* method. The second test case, shown in Section 3.2, is a Poiseuille-Graetz problem [16, 25].

From here on, we will explicitly write the FE space dimension $\mathcal{N}$ only when it will be necessary.

3.1. A first test case

We begin by studying a problem depending only on one "physical" parameter, actually the global Péclet number. Let Ω be the unit square in $\mathbb{R}^2$, that is $(0,1) \times (0,1)$. The domain is sketched in Figure 1. The problem is the following one:

$$\begin{cases} -\dfrac{1}{\mu}\Delta u(\mu) + (1,1) \cdot \nabla u(\mu) = 0 & \text{in } \Omega \\ u(\mu) = 0 & \text{on } \Gamma_1 \cup \Gamma_2 \\ u(\mu) = 1 & \text{on } \Gamma_3 \cup \Gamma_4 \end{cases} \tag{15}$$

with $\mu > 0$. Note that μ is the Péclet number of our problem, so we will be interested in the case in which μ is high (as $\boldsymbol{\mu}$ is now a scalar, in this Section we identify $\boldsymbol{\mu}$ and μ).

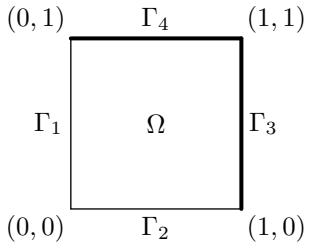

Figure 1: First test case: domain. On the bold sides we impose $u = 1$, while on the rest of the boundary $u = 0$.

Let $\mathcal{T}_h$ be a proper triangulation of Ω. We define $X^{\mathcal{N}}$ as the subspace of $\mathbb{P}^r(\mathcal{T}_h) = \{v_h \in H^1(\Omega) \,|\, v_h|_K \in \mathbb{P}^r(K), K \in \mathcal{T}_h\}$ made up by the functions that vanish on the boundary of Ω.

A very interesting case is when the local Péclet number fulfils condition (12). In Figure 2 the solution obtained by using a non-stabilized FE approximation with $\mu = 600$ is represented. In this case we can perform a RB approximation of the solution, but the RB solutions reflect all the instability problems of the FE solution, as we can see in Figure 3. For this simple case, if we let the parameter range from 100 to 1000 the Greedy algorithm converges and the energy norm of the difference between the RB solution and the FE solution behaves as for lower values of the Péclet number, as we can see in Figure 4, but this procedure would lead us to wrong physical results. This happens because the target of the RB approach is to approximate the exact continuous solution of the problem by trying to recover the FE solution which is not a stable approximation of the exact one, in this case. The vertical dotted lines in Figure 3 are plotted in correspondence of the parameter values selected by the greedy algorithm [25]. It is evident that the RB approximation error vanishes in correspondence of the parameter values selected by the greedy algorithm, as expected by definition of RB solution to guarantee the consistency of the method and the reconstruction of one of the basis solutions.

A possible way to fix this instability problems could be to use some stabilization methods. We chose to use the SUPG stabilization method. This consists in adding a strongly consistent

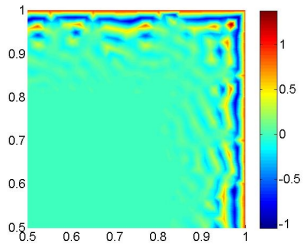

Figure 2: First test case, high Péclet number. FE solution for $\mu = 600$ (zoom on $[0.5, 1] \times [0.5, 1]$).

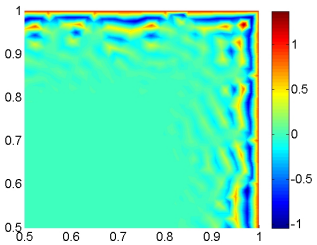

Figure 3: First test case, high Péclet number. RB solution for for $\mu = 600$ (zoom on $[0.5, 1] \times [0.5, 1]$).

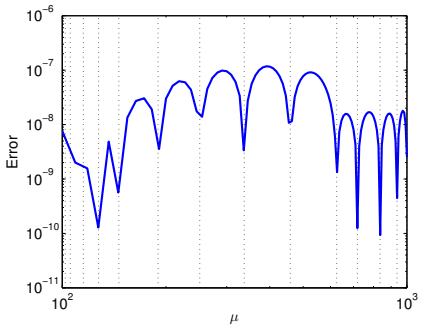

Figure 4: First test case, high Péclet number. RB approximation error expressed as a function of the parameter

stabilization term to the bilinear form a associated to the continuous problem, that is

$$a(w, v; \mu) := \int_\Omega \frac{1}{\mu} \nabla w \cdot \nabla v + (\partial_x w + \partial_y w)\, v. \tag{16}$$

We chose to use $\mathbb{P}^1$ finite elements, that is $r = 1$. As piecewise linear functions have null Laplacian on each element K, the SUPG stabilization term reduces to:

$$s(w_h, v_h; \mu) = \sum_{K \in \mathcal{T}_h} \frac{\delta_K h_K}{\sqrt{2}} \int_K (\partial_x w_h + \partial_y w_h)(\partial_x v_h + \partial_y v_h) \tag{17}$$

again with $w_h, v_h \in \mathbb{P}^1(\mathcal{T}_h)$. Note that, in this case, the stabilization term (17) is actually parameter independent. As regards the right hand side, denoting with g_h a lifting of the Dirichlet boundary conditions, we define $F(v^{\mathcal{N}}; \mu) := -a(g_h, v^{\mathcal{N}}; \mu)$ and $F^s(v^{\mathcal{N}}) := -s(g_h, v^{\mathcal{N}})$. The final stabilized FE formulation is

$$\begin{aligned} &\text{find } u^{\mathcal{N}}(\mu) \in X^{\mathcal{N}} \text{ s.t.} \\ &a_{stab}(u^{s\,\mathcal{N}}(\mu), v^{\mathcal{N}}; \mu) = F_{stab}(v^{\mathcal{N}}; \mu) \quad \forall v^{\mathcal{N}} \in X^{\mathcal{N}}. \end{aligned} \tag{18}$$

where

$$a_{stab} = a + s, \qquad F_{stab} = F + F^s. \tag{19}$$

It is straightforward to prove that, for our choice of polynomial approximation space, we do not need to fulfil any requirement on the weights δ_K to guarantee the stability of the discrete

problem (18) with respect to the SUPG norm [27]:

$$\|v^{\mathcal{N}}\|^2_{SUPG,\boldsymbol{\mu}} = |||v^{\mathcal{N}}|||^2_{\boldsymbol{\mu}} + \sum_{K\in\mathcal{T}_h} \delta_K \left(L_{SS} v^{\mathcal{N}}, \frac{h_K}{|\boldsymbol{\beta}(\boldsymbol{\mu})|} L^{\boldsymbol{\mu}}_{SS} v^{\mathcal{N}} \right)_K \qquad \forall v^{\mathcal{N}} \in X^{\mathcal{N}}, \quad \forall \boldsymbol{\mu} \in \mathcal{D}, \tag{20}$$

simply because this is actually the norm induced by $a_{stab}(\cdot,\cdot;\boldsymbol{\mu})$ on $X^{\mathcal{N}}$. In (20) $|||\cdot|||_{\boldsymbol{\mu}}$ is the norm induced by the symmetric part of the advection-diffusion operator that is

$$|||v|||^2_{\boldsymbol{\mu}} = \int_\Omega \varepsilon(\boldsymbol{\mu}) \, |\nabla v|^2, \quad \forall v \in H^1_0(\Omega), \tag{21}$$

while $L^{\boldsymbol{\mu}}_{SS}$ is the skew-symmetric part of the advection-diffusion operator, defined in (3). We then set $\delta_K = 1$ for each element $K \in \mathcal{T}_h$.

Now we can try the two different approaches described before: the *Offline-Online stabilized* and the *Offline-only stabilized* methods. As regards the first one, we have just to perform the whole RB standard method simply using a_{stab} instead of a. The *Offline-only stabilized* approach consists in using the form a_{stab} during the Offline stage, in order to obtain stable reduced basis, and to perform the Online Galerkin projection with respect to the form a. Formally, denoted by $X^{\mathcal{N}}_N$ the space spanned by the reduced basis, the *Offline-Online stabilized* solution $u^s_N(\mu) \in X^{\mathcal{N}}_N$ satisfies

$$a_{stab}(u^s_N(\mu), v_N; \mu) = F_{stab}(v_N; \mu) \quad \forall\, v_N \in X^{\mathcal{N}}_N \tag{22}$$

while the *Offline-only stabilized* solution $u_N(\mu) \in X^{\mathcal{N}}_N$ is such that

$$a(u_N(\mu), v_N; \mu) = F(v_N; \mu) \quad \forall\, v_N \in X^{\mathcal{N}}_N. \tag{23}$$

By using the norm induced by a_{stab} to carry out the Offline stage, we are actually taking the SUPG stabilized FE solution $u^{s\,\mathcal{N}}(\mu)$ as the "exact" one. So it makes sense to measure the performance of the method by evaluating the difference between the RB solution and the stabilized FE one.

The *Offline-Online stabilized* method, as expected, produces stable RB solutions, as shown in Figure 5a, and the actual error, with respect to the stabilized FE solution, is smaller than the tolerance guaranteed by the greedy algorithm ($\varepsilon^*_{tol} = 10^{-5}$), as we can see in Figure 6. On the contrary, the behaviour of the *Offline-only stabilized* approach is very unsatisfactory. As we can see in Figure 5b, even though the reduced basis are stable, the *Offline-only stabilized* RB solutions show large oscillations. *We have actually shown that a Galerkin projection on a subspace spanned by stable functions does not guarantee a stable solution for large values of the Péclet number.*

In order to better understand which are the causes of the instability of the *Offline-only stabilized* method, we try to use a locally refined mesh to build the reduced basis, instead of the SUPG stabilization method, during the Offline stage. In this case, "locally" means that we refine the mesh in the area in which we expect that the boundary layer will arise. Acting in this way, we can obtain Offline stable reduced basis without resorting to any stabilization method, because the condition (12) is no more satisfied, at least where we previously had instability problems. Obviously, by increasing the number of degrees of freedom, we quite increase the computational cost. The Offline algorithm, performed using the refined mesh and the original bilinear form, produces 14 basis and it takes 711 seconds while the Offline algorithm, carried out with the coarser mesh and the stabilized bilinear form, takes only 114 seconds and builds 8 basis. The RB solutions obtained for the same parameter range as before do not show instability phenomena, so an explanation of the behaviour of the *Offline-only stabilized* method tested before has to be found analysing the use of different bilinear forms in the two stages of the RB method, as we will do further. We can underline how a stabilization technique performs computationally better than a local refinement technique.

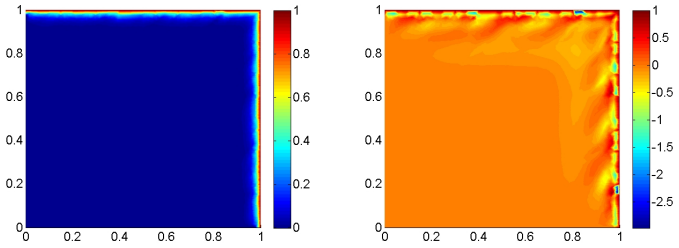

(a) *Offline-Online stabilized* (b) *Online-only stabilized*

Figure 5: First test case, high Péclet number. *Offline-Online stabilized* and *Offline-only stabilized* RB solutions for $\boldsymbol{\mu} = 600$ (zoom on $[0.5, 1] \times [0.5, 1]$).

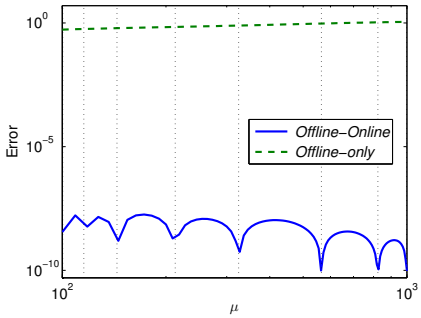

Figure 6: First test case, high Péclet number. comparison of the RB approximation error obtained for the two different stabilization strategies. Here the error is expressed as a function of the parameter. The vertical dotted lines are plotted in correspondence of the parameters values selected by the Greedy algorithm.

3.2. A second test case: Poiseuille-Graetz flow

We now focus on a different situation, a Graetz problem [9, 16, 25, 31], in which we have two parameters: a physical one (the Péclet number) and a geometrical one (the length of the domain). The Graetz problem deals with steady forced heat convection (advective phenomenon) combined with heat conduction (diffusive phenomenon) in a duct with walls at different temperature. Let us define $\boldsymbol{\mu} = (\mu_1, \mu_2)$ where both μ_1 and μ_2 are positive real numbers. Let $\Omega_o(\boldsymbol{\mu})$ be the rectangle $(0, 1 + \mu_2) \times (0, 1)$ in $\mathbb{R}^2$. The domain is shown in Figure 7.

The problem is to find a solution $u(\boldsymbol{\mu})$, representing the temperature distribution, such that:

$$\begin{cases} -\dfrac{1}{\mu_1}\Delta u(\boldsymbol{\mu}) + 4\,y(1-y)\partial_x u(\boldsymbol{\mu}) = 0 & \text{in } \Omega_o(\boldsymbol{\mu}) \\ u(\boldsymbol{\mu}) = 0 & \text{on } \Gamma_{o\,1}(\boldsymbol{\mu}) \cup \Gamma_{o\,2}(\boldsymbol{\mu}) \cup \Gamma_{o\,6}(\boldsymbol{\mu}) \\ u(\boldsymbol{\mu}) = 1 & \text{on } \Gamma_{o\,3}(\boldsymbol{\mu}) \cup \Gamma_{o\,5}(\boldsymbol{\mu}) \\ \dfrac{\partial u}{\partial \nu} = 0 & \text{on } \Gamma_{o\,4}(\boldsymbol{\mu}). \end{cases} \tag{24}$$

We set a reference domain $\Omega = (0, 2) \times (0, 1)$ subdivided into subdomains $\Omega^1 = (0, 1) \times (0, 1)$ and $\Omega^2 = (1, 2) \times (0, 1)$. The affine transformation that maps the reference domain into the original one [25, 29], are:

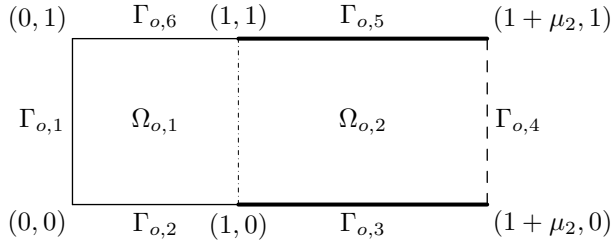

Figure 7: Poiseuille-Graetz test case problem: parametrized domain. Boundary conditions: $u = 1$ on the bold sides, homogeneous Neumann on the dashed side and homogeneous Dirichlet on the remaining boundary sides.

$$
\begin{aligned}
&T^1(\boldsymbol{\mu})\colon \Omega^1 \to \mathbb{R}^2, && T^2(\boldsymbol{\mu})\colon \Omega^2 \to \mathbb{R}^2,\\
&T^1\left(\begin{pmatrix}x\\y\end{pmatrix};\boldsymbol{\mu}\right) = \begin{pmatrix}x\\y\end{pmatrix}, && T^2\left(\begin{pmatrix}x\\y\end{pmatrix};\boldsymbol{\mu}\right) = \begin{pmatrix}\mu_2 & 0\\0 & 1\end{pmatrix}\begin{pmatrix}x\\y\end{pmatrix} - \begin{pmatrix}1-\mu_2\\0\end{pmatrix},
\end{aligned}
$$

If we glue together these two transformations, for each $\boldsymbol{\mu} \in \mathcal{D}$ we actually define a transformation $T(\boldsymbol{\mu})$ of the whole domain Ω. Note that $T(\boldsymbol{\mu})$ is a continuous one-to-one transformation.

Let us now define a mesh $\mathcal{T}_h$ on the reference domain Ω and let us call $\mathcal{T}_h^1$ and $\mathcal{T}_h^2$ the restrictions $\mathcal{T}_h$ to Ω_1 and Ω_2, respectively. We can also define a mesh on $\Omega_o(\boldsymbol{\mu})$ just by taking the image of $\mathcal{T}_h$ through the transformation $T(\cdot, \boldsymbol{\mu})$, that is $\mathcal{T}_{h,o}(\boldsymbol{\mu}) = \{K_o(\boldsymbol{\mu}) = T(K;\boldsymbol{\mu}) \mid K \in \mathcal{T}_h\}$. We define the stabilization term, for the $\mathbb{P}^1$-FE case, to be added to the left-hand side of the FE formulation of the problem:

$$
s(w_h, v_h; \boldsymbol{\mu}) := \sum_{K_o(\boldsymbol{\mu}) \in \mathcal{T}_{h,o}(\boldsymbol{\mu})} \delta_{K_o(\boldsymbol{\mu})} \int_{K_o(\boldsymbol{\mu})} h_{K_o(\boldsymbol{\mu})} \left(4\, y(1-y)\right)^2 \partial_x w_h \partial_x v_h. \tag{25}
$$

Once tracked back onto the reference domain the involved bilinear forms turn out to be:

$$
\begin{aligned}
a(w_h, v_h; \boldsymbol{\mu}) := &\int_{\Omega^1} \frac{1}{\mu_1} \nabla w_h \cdot \nabla v_h + 4\, y(1-y) \partial_x w_h\, v_h\\
&+ \int_{\Omega^2} \frac{1}{\mu_1 \mu_2} \partial_x w_h \partial_x v_h + \frac{\mu_2}{\mu_1} \partial_y w_h \partial_y v_h\\
&\qquad + 4\, y(1-y) \partial_x w_h\, v_h
\end{aligned} \tag{26}
$$

and:

$$
\begin{aligned}
s(w_h, v_h; \boldsymbol{\mu}) := &\sum_{K \in \mathcal{T}_h^1} h_K \int_K \left(4\, y(1-y)\right)^2 \partial_x w_x \partial_x v_h\\
&+ \sum_{K \in \mathcal{T}_h^2} \frac{h_K}{\mu_2} \sqrt{\frac{1+\mu_2^2}{2}} \int_K \left(4\, y(1-y)\right)^2 \partial_x w_x \partial_x v_h.
\end{aligned} \tag{27}
$$

By introducing a lifting of the Dirichlet boundary condition we can obtain the stabilized FE formulation (18), as we did in Section 3.1. We point out that for $K \in \mathcal{T}_h^2$ we are choosing $\delta_{K_o(\boldsymbol{\mu})}$ such that $\delta_{K_o(\boldsymbol{\mu})}\, h_{K_o(\boldsymbol{\mu})} \approx h_K \sqrt{(1+\mu_2^2)/2}$, assuming that each element diameter transforms as the diameter of the whole subdomain. This rescaling is done mainly for preserving the convergence rate of the SUPG method. We need to make an assumption like this also because it would make no

sense, in an RB point of view, to compute Online every exact value of $h_{K_o(\boldsymbol{\mu})}$. Indeed, the Online stage of the RB method actually is independent of the triangulation $\mathcal{T}_h$.

As pointed out in [8], if the advection dominated condition (12) is not fulfilled for all $K \in \mathcal{T}$ we locally lose even the h^r convergence rate of the standard FE method. A possible way to overcome this trouble is to act on the weights δ_K, distinguishing between the elements for which $\mathbb{P}\mathrm{e}_K > 1$ and $\mathbb{P}\mathrm{e}_K \leq 1$. We want to observe that, unfortunately, by using a weighting that depends on both parameter and element size we lose the affinity assumption (4) on the bilinear form, or better, we lose that assumption with a number of affine terms Q_a independent of $\mathcal{N}$. So, if we are facing problems in which the advection dominated condition (12) is not fulfilled for all $K \in \mathcal{T}_h$ and we want to rigorously recover the convergence order of the FE method, in order to resort to a weighting $\delta = \delta(\boldsymbol{x}, \boldsymbol{\mu})$ (as proposed in [8]) we need to exploit some interpolation techniques involving the empirical interpolation [1][2]. In this case it would be also worth to check if it were possible to define a weighting that does not depend on each h_K, but on the mesh size $h = \max_{K \in \mathcal{T}_h} h_k$, under suitable regularity assumptions [19].

We would like also to recall that the convergence performances of the stabilization method depend on the regularity properties of the mesh. So, as the meshes $\mathcal{T}_{h,o}(\boldsymbol{\mu})$ we are actually using to stabilize on the original domains are the image through T of the triangulation defined on the reference domain, we should guarantee that the transformation T does not worsen the properties of the reference triangulation. In our numerical tests the reference domain will be the one corresponding to $\mu_2 = 1$ and we will let the parameter range from 0.5 to 4, so we will not have an excessive deformation. We will also use a quite coarse mesh (mesh size $h = 0.06$) and high values for μ_1 (from 10000 to 20000) in order to have significant instability problems. The point is that the boundary layer arises in an area in which the norm of the advection field (an thus the value of the local Péclet number) is relatively small. In Figure 8 we show the average local Péclet number computed on each element of the mesh. We would like to point out that even if the advection field vanishes as we get close to the boundary, the average local Péclet number is greater than 1. The lowest value assumed by the average local Péclet number is 3.23, while the highest is 151.

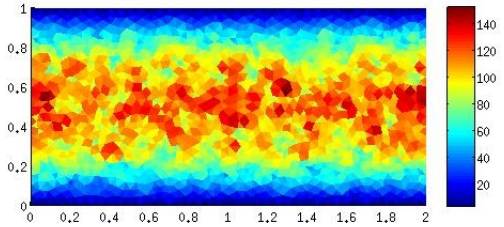

Figure 8: Poiseuille-Graetz test case. Average local Péclet number computed on each element of the mesh.

In Figures 9a and 9b we show the RB obtained respectively by *Offline-Online stabilized* method and by *Offline-only stabilized* method, for $\boldsymbol{\mu} = (12500, 3)$.

Finally, in Figure 10 we show the error curves of the two methods. As in the previous test-case, we can see that only the *Offline-Online stabilized* produces satisfactory results, even if now the *Offline-only stabilized* method has slightly better performances than in the previous test case. We used a parameter domain $\mathcal{D} = [10000, 20000] \times [0.5, 4]$ and a truth space of dimension $\mathcal{N} = 1309$. The tolerance[3] on the Greedy algorithm is $\varepsilon^*_{tol} = 10^{-3}$. The Greedy algorithm produced $N = 15$

[2]We have to remark that the weighting proposed in [8] is discontinuous in both $\boldsymbol{x}$ and $\boldsymbol{\mu}$ even if the coefficients ε and $\boldsymbol{\beta}$ are smooth.

[3]The tolerance is on the stabilized energy norm, that is greater than the non-stabilized one (see (28)).

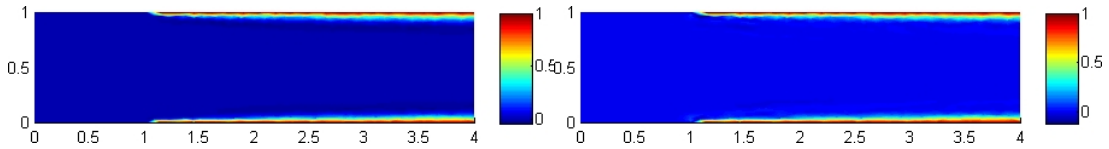

(a) *Offline-online stabilized* (b) *Offline-only stabilized*

Figure 9: Poiseuille-Graetz test case. *Offline-Online stabilized* and *Offline-only stabilized* RB solutions for $\boldsymbol{\mu} = (12500, 3)$.

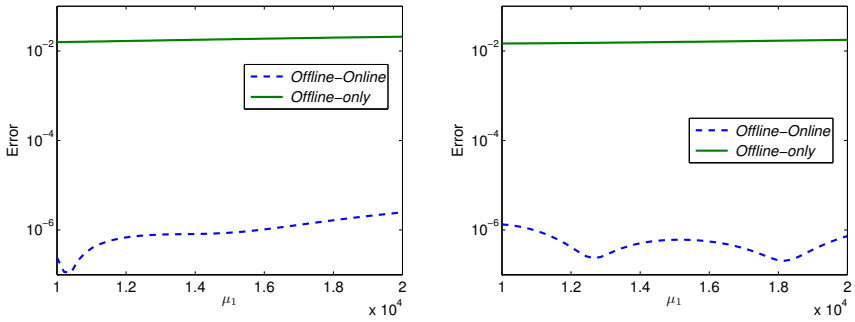

(a) $\mu_2 = 2.5$ (b) $\mu_2 = 3.5$

Figure 10: Poiseuille-Graetz test case. Comparison of the RB approximation error obtained for the two different stabilization strategies; here the error is expressed as a function of the parameter μ_1, given a value of μ_2.

basis and the computational time of the whole Offline stage was 254 s.

3.3. Discussions on the results

Observing the results obtained up to now, it seems that the best way to perform stabilization is the *Offline-Online stabilized* one. But let us try to understand why the *Offline-only stabilized* option has a bad behaviour.

Let us introduce some notation. Let us call *energy norm* the norm on $H_0^1(\Omega(\boldsymbol{\mu}))$ induced by the symmetric part of the advection diffusion operator a and *stabilized energy norm* the one induced by the symmetric part of a_{stab}. In symbols:

$$|||\cdot|||_{\boldsymbol{\mu}} = \sqrt{a^{sym}(\cdot,\cdot;\boldsymbol{\mu})}, \qquad |||\cdot|||_{\boldsymbol{\mu},stab} = \sqrt{a^{sym}_{stab}(\cdot,\cdot;\boldsymbol{\mu})}. \tag{28}$$

First of all we have to note that by performing the Offline stage using the stabilized operator and the standard *a posteriori* error estimators, we are actually assuring that the "reliable" RB approximation is the *Offline-Online stabilized* one. This is because the Greedy algorithm [25, 29] (performed using the stabilized form a_{stab}) guarantees that

$$|||u^s_N(\boldsymbol{\mu}) - u^{s\,\mathcal{N}}(\boldsymbol{\mu})|||_{\boldsymbol{\mu},stab} \leq \varepsilon^*_{tol} \quad \forall \boldsymbol{\mu} \in \Xi_{train} \subset \mathcal{D} \tag{29}$$

where $u^s_N(\boldsymbol{\mu})$ is the *Offline-Online stabilized* solution, $u^{s\,\mathcal{N}}(\boldsymbol{\mu})$ is the stabilized FE solution and Ξ_{train} is the training set introduced in Section 2.2. So the Offline procedure actually allows us to control only the error committed by the *Offline-Online stabilized* method.

Thus we have to find some estimates for the difference in norm between the *Offline-only stabilized* solution $u_N(\boldsymbol{\mu})$ and the FE stabilized one $u^{s\,\mathcal{N}}(\boldsymbol{\mu})$. We can try by splitting the difference in this way:

$$|||u_N(\boldsymbol{\mu}) - u^{s\,\mathcal{N}}(\boldsymbol{\mu})|||_{\boldsymbol{\mu}} \leq |||u_N(\boldsymbol{\mu}) - u_N^s(\boldsymbol{\mu})|||_{\boldsymbol{\mu}} + |||u_N^s(\boldsymbol{\mu}) - u^{s\,\mathcal{N}}(\boldsymbol{\mu})|||_{\boldsymbol{\mu}}. \tag{30}$$

Of course, it holds that

$$|||u_N^s(\boldsymbol{\mu}) - u^{s\,\mathcal{N}}(\boldsymbol{\mu})|||_{\boldsymbol{\mu}} \leq |||u_N^s(\boldsymbol{\mu}) - u^{s\,\mathcal{N}}(\boldsymbol{\mu})|||_{\boldsymbol{\mu},stab} \leq \varepsilon_{tol}^*, \tag{31}$$

therefore we have to provide an estimate of the distance with respect to the energy norm between $u_N(\boldsymbol{\mu})$ and $u_N^s(\boldsymbol{\mu})$. To do so we can simply start from the definition:

$$\begin{aligned} |||u_N(\boldsymbol{\mu}) - u_N^s(\boldsymbol{\mu})|||_{\boldsymbol{\mu}}^2 =& a(u_N(\boldsymbol{\mu}) - u_N^s(\boldsymbol{\mu}), u_N(\boldsymbol{\mu}) - u_N^s(\boldsymbol{\mu}); \boldsymbol{\mu}) \\ =& - F^s(u_N(\boldsymbol{\mu}) - u_N^s(\boldsymbol{\mu}); \boldsymbol{\mu}) + s(u_N^s(\boldsymbol{\mu}), u_N(\boldsymbol{\mu}) - u_N^s(\boldsymbol{\mu}); \boldsymbol{\mu}) \\ =& s(u_N^s(\boldsymbol{\mu}) + g_h, u_N(\boldsymbol{\mu}) - u_N^s(\boldsymbol{\mu}); \boldsymbol{\mu}), \end{aligned} \tag{32}$$

where g_h is the lifting of the Dirichlet boundary data (recall also relations (19)). For the SUPG stabilization with $\mathbb{P}^1$ elements, the following bound holds:

$$\begin{aligned} |s(u_N^s(\boldsymbol{\mu}) + g_h, u_N(\boldsymbol{\mu}) - u_N^s(\boldsymbol{\mu}))| \leq& h_{max}(\boldsymbol{\mu}) \, \|\boldsymbol{\beta}(\boldsymbol{\mu}) \cdot \nabla(u_N^s(\boldsymbol{\mu}) + g_h)\|_{L^2(\Omega_o(\boldsymbol{\mu}))} \\ & \cdot \left\| \frac{\boldsymbol{\beta}(\boldsymbol{\mu})}{|\boldsymbol{\beta}(\boldsymbol{\mu})|} \cdot \nabla(u_N(\boldsymbol{\mu}) - u_N^s(\boldsymbol{\mu})) \right\|_{L^2(\Omega_o(\boldsymbol{\mu}))} \\ \leq& h_{max}(\boldsymbol{\mu}) \, \|\boldsymbol{\beta}(\boldsymbol{\mu}) \cdot \nabla(u_N^s(\boldsymbol{\mu}) + g_h)\|_{L^2(\Omega_o(\boldsymbol{\mu}))} \\ & \cdot |u_N(\boldsymbol{\mu}) - u_N^s(\boldsymbol{\mu})|_{H_0^1(\Omega_o(\boldsymbol{\mu}))}. \end{aligned}$$

where $h_{max}(\boldsymbol{\mu}) = \max_{K \in \mathcal{T}_h} h_{K_o(\boldsymbol{\mu})}$. As the energy norm is equivalent to $|\cdot|_{H_0^1}$, we have that:

$$|v|_{H_0^1(\Omega_o(\boldsymbol{\mu}))} \leq C(\boldsymbol{\mu}) \, |||v|||_{\boldsymbol{\mu}} \quad \forall v \in H_0^1(\Omega_o(\boldsymbol{\mu})). \tag{33}$$

We can also bound the L^2-norm of the streamline derivative of the *Offline-Online* stabilized RB solution with that of the FE stabilized solution:

$$\begin{aligned} \|\boldsymbol{\beta}(\boldsymbol{\mu}) \cdot \nabla(u_N^s(\boldsymbol{\mu}) + g_h)\|_{L^2(\Omega_o(\boldsymbol{\mu}))} \leq& \|\boldsymbol{\beta}(\boldsymbol{\mu}) \cdot \nabla(u^{s\,\mathcal{N}}(\mu) + g_h)\|_{L^2(\Omega_o(\boldsymbol{\mu}))} \\ & + \|\boldsymbol{\beta}(\boldsymbol{\mu}) \cdot \nabla(u_N^s(\boldsymbol{\mu}) - u^{s\,\mathcal{N}}(\boldsymbol{\mu}))\|_{L^2(\Omega_o(\boldsymbol{\mu}))} \\ \leq& \|\boldsymbol{\beta}(\boldsymbol{\mu}) \cdot \nabla(u^{s\,\mathcal{N}}(\mu) + g_h)\|_{L^2(\Omega_o(\boldsymbol{\mu}))} + C(\boldsymbol{\mu}) \|\boldsymbol{\beta}(\boldsymbol{\mu})\|_{L^\infty(\Omega_o(\boldsymbol{\mu}))} \varepsilon_{tol}^*. \end{aligned} \tag{34}$$

We note that this argument allows us to prove the inequalities shown in the following proposition, that are upper bound for the distance with respect to the energy norm between $u_N(\boldsymbol{\mu})$ and $u^{s\,\mathcal{N}}(\boldsymbol{\mu})$. The first one is a proper *a priori* upper bound, while the second one is a sharper bound, but not properly *a priori*.

Proposition 3.1 (Error bounds for the *Offline-only stabilized* method)**.** *The following estimates of the error between the Offline-only stabilized approximation $u_N(\boldsymbol{\mu})$ and the stabilized FE approximation $u^{s\,\mathcal{N}}(\boldsymbol{\mu})$ hold:*

$$\begin{aligned} |||u_N(\boldsymbol{\mu}) - u^{s\,\mathcal{N}}(\boldsymbol{\mu})|||_{\boldsymbol{\mu}} \leq& h_{max}(\boldsymbol{\mu}) C(\boldsymbol{\mu}) \|\boldsymbol{\beta}(\boldsymbol{\mu}) \cdot \nabla(u^{s\,\mathcal{N}}(\boldsymbol{\mu}) + g_h)\|_{L^2(\Omega_o(\boldsymbol{\mu}))} \\ & + \left(1 + h_{max}(\boldsymbol{\mu}) C(\boldsymbol{\mu})^2 \|\boldsymbol{\beta}(\boldsymbol{\mu})\|_{L^\infty(\Omega_o(\boldsymbol{\mu}))}\right) \varepsilon_{tol}^*. \end{aligned} \tag{35}$$

$$\begin{aligned} |||u_N(\boldsymbol{\mu}) - u^{s\,\mathcal{N}}(\boldsymbol{\mu})|||_{\boldsymbol{\mu}} \leq& h_{max}(\boldsymbol{\mu}) \, C(\boldsymbol{\mu}) \|\boldsymbol{\beta}(\boldsymbol{\mu}) \cdot \nabla(u_N^s(\boldsymbol{\mu}) + g_h)\|_{L^2(\Omega_o(\boldsymbol{\mu}))} \\ & + |||u_N^s(\boldsymbol{\mu}) - u^{s\,\mathcal{N}}(\boldsymbol{\mu})|||_{\boldsymbol{\mu}}. \end{aligned} \tag{36}$$

where $u_N^s(\boldsymbol{\mu})$ is the Offline-Online stabilized solution and g_h is the lifting of the Dirichlet boundary condition. $C(\boldsymbol{\mu})$ is the norm equivalence constant defined in (33) *and $h_{max}(\boldsymbol{\mu})$ is the maximum element diameter of the mesh defined on the parametric domain.*

Remark 3.1. We point out that the bound in (35) depends on the L^2 norm of the streamline derivative of the stabilized solution (with the non homogeneous Dirichlet boundary conditions). *This means that the Offline-only stabilized method has better performances when applied to problems in which the strongest variations occur along a direction orthogonal to the advection field. This could happen in the cases in which the boundary layers are parallel to the advection field, e.g. the Poiseuille-Graetz problem.* The "improvement" of the approximation is confirmed by comparing the numerical results shown in Figures 6 and 10.

We performed some numerical tests for the bound in (36). The results are shown in Figures 11 and 12. Concerning the first test case we set $C(\mu) = \sqrt{\mu}$ and for the Poiseuille-Graetz problem: $C(\boldsymbol{\mu}) = \sqrt{\mu_1}$. With these choices, (33) is actually an equality.

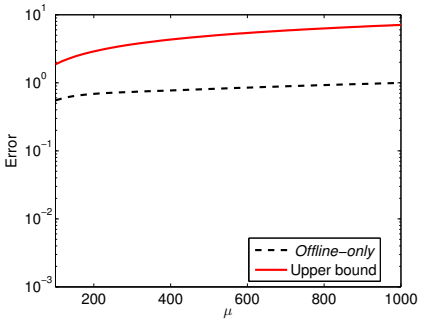

Figure 11: First test case. Upper bound (36) compared to the true error

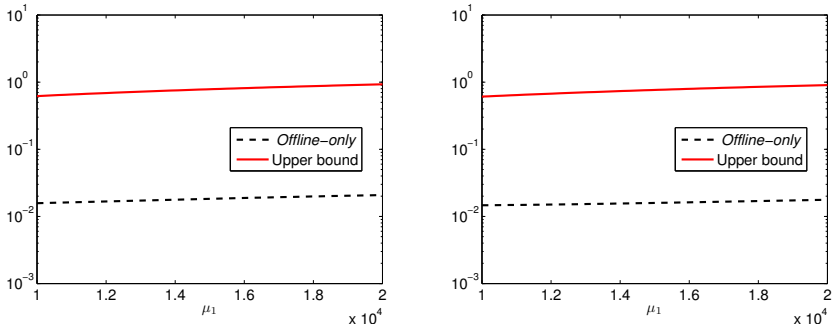

(a) $\mu_2 = 2.5$ (b) $\mu_2 = 3.5$

Figure 12: Poiseuille-Graetz test case. Upper bound (36) compared to the true error.

We can see that the bound is sharp in the first test case, while in the Graetz problem the bound tends to overestimate the real error by two orders of magnitude.

The reasonable sharpness of the error bound obtained for at least one test case leads us to state that the *Offline-only stabilized* approach is not a good approximation method.

Even if the *Offline-only stabilized* is strongly consistent with respect to the continuous problem, we have to note that we actually have a "consistency" problem caused by the use of different bilinear forms in the two stages. One problem is that the Offline stage, as described in [25, 29], is tailored to minimize the error between the *Offline-Online stabilized* solution and the stabilized FE one. This implies that, during the Offline stage, we are not controlling the approximation error of the *Offline-only stabilized* solution, causing the "inconsistency", bounded from above by the streamline

derivative term in (35) and (36). The reasonable sharpness obtained in one test case suggests that the streamline derivative term can actually be a major responsible of the difference between the Offline-only stabilized solution and the Offline-online stabilized one.

3.3.1. Effectivity of the a posteriori error estimator for the Offline-Online stabilized method

In order to further assess the performances of the *Offline-Online stabilized* method, we want to study the effectivity of the error estimators for the Online stage.

We recall that the *Offline-Online stabilized* method is a particular case of the RB method for elliptic problems, in which we consider as bilinear form the stabilized one. So we can exploit the already existing theory for the *a posteriori* estimation of the error. Following [25, 29], we define the *effectivity* of the error estimator $\Delta_{N,stab}$ as:

$$\eta_{N,stab}(\boldsymbol{\mu}) = \frac{\Delta_{N,stab}(\boldsymbol{\mu})}{|||u^{s\,\mathcal{N}}(\boldsymbol{\mu}) - u_N^s(\boldsymbol{\mu})|||_{\boldsymbol{\mu},stab}} \quad \forall \boldsymbol{\mu} \in \mathcal{D}. \tag{37}$$

In our numerical tests, we considered a set $\Xi_{test} \subset \mathcal{D}$ of about 100 elements and then we computed the average efficiency $\eta^{av}_{N,stab} = \frac{1}{|\Xi_{test}|} \sum_{\boldsymbol{\mu} \in \Xi_{test}} \eta_{N,stab}(\boldsymbol{\mu})$.

In Table 1 we show the results obtained for both the first test case and the Poiseuille-Graetz problem. We can observe that the effectivity is small and this means that the error estimator does not provide unnecessary overly conservative estimates.

Test case	$\lvert\Xi_{test}\rvert$	$\eta^{av}_{N,stab}$
First test case	101	8.37
Poiseuille-Graetz	126	6.59

Table 1: First test case and Poiseuille-Graetz test case. Average effectivities in numerical tests

4. Stabilized reduced basis: parameter dependent internal layer

In the previous Section our aim was to study a good stabilization strategy for the RB method and it turned out that the *Offline-Online* method seems to be a good choice. In this section we want to test our stabilization method with a problem characterized by the presence of an internal layer whose direction depends on the parameter. This problem was also used in [3]. We also try the stabilization method using a different truth space, i.e. piecewise quadratic polynomials. Let Ω be the unit square in $\mathbb{R}^2$, as sketched in Figure 13, and let us define $\boldsymbol{\mu} = (\mu_1, \mu_2)$, where $\mu_1, \mu_2 \in \mathbb{R}$. The problem is the following one:

$$\begin{cases} -\dfrac{1}{\mu_1}\Delta u(\boldsymbol{\mu}) + (\cos\mu_2, \sin\mu_2) \cdot \nabla u(\boldsymbol{\mu}) = 0 & \text{in } \Omega \\ u(\boldsymbol{\mu}) = 1 & \text{on } \Gamma_1 \cup \Gamma_2 \\ u(\boldsymbol{\mu}) = 0 & \text{on } \Gamma_3 \cup \Gamma_4 \cup \Gamma_5. \end{cases} \tag{38}$$

Let us note that μ_1 represents the Péclet number of the advection-diffusion problem, while μ_2 is the angle between the x axis and the direction of the constant advection field. The bilinear form associated to the problem is:

$$a(w, v; \boldsymbol{\mu}) = \int_\Omega \frac{1}{\mu_1} \nabla w \cdot \nabla v + (\cos\mu_2\, \partial_x w + \sin\mu_2\, \partial_y w) v. \tag{39}$$

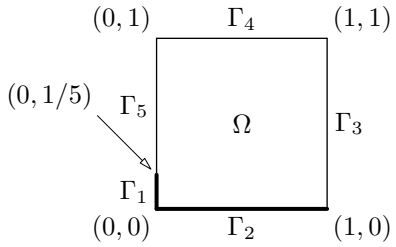

Figure 13: Higher order polynomial approximation. Domain of the problem (38). On the bold sides we impose $u = 1$, while on the other ones $u = 0$.

We introduce again a triangulation $\mathcal{T}_h$ on the domain Ω and we consider $\mathbb{P}^r(\mathcal{T}_h)$, that is the piecewise polynomial interpolation space of order r ($r = 1, 2$). Now we can define, for $r = 1, 2$, our stabilization term:

$$\begin{aligned} s^r(w_h, v_h; \boldsymbol{\mu}) = &- \sum_{K \in \mathcal{T}_h} h_K \, \delta_K^r \int_K \frac{1}{\mu_1} \Delta w_h \; (\cos\mu_2, \sin\mu_2) \cdot \nabla v_h \\ &+ \sum_{K \in \mathcal{T}_h} h_K \, \delta_K^r \int_K (\cos\mu_2, \sin\mu_2) \cdot \nabla w_h \; (\cos\mu_2, \sin\mu_2) \cdot \nabla v_h, \end{aligned} \tag{40}$$

in which the value of the weights δ_K^r is to be assigned. Note that if $r = 1$ the first sum is null, because piecewise linear functions have null Laplacian on each element K.

As regards the weights δ_K^r, we made different choice for the two different polynomial order. As we saw in Section 3, if $r = 1$ we do not have any restriction on the weights, so we choose $\delta_K^1 = 1 \quad \forall K \in \mathcal{T}_h$.

On the contrary, if $r = 2$, we recall that the weights δ_K^2 have to be sufficiently small to guarantee the stability with respect to the SUPG norm (20), as shown in [8, 27]. We set $\delta_K^2 = \frac{1}{2}$ for each element K, following the choice proposed in [8]. As in the latter work, we consider following definition of the local Péclet number:

$$\mathbb{P}\mathrm{e}_K(\boldsymbol{\mu}) = \frac{|\boldsymbol{\beta}(\boldsymbol{\mu})| h_K}{C_2 \, \varepsilon(\boldsymbol{\mu})} \quad \forall \boldsymbol{\mu} \in \mathcal{D}, \tag{41}$$

where h_K is the element size redefined as

$$h_K^2 = \frac{4 A_K}{\sqrt{3 \sum_{i=1}^3 |\boldsymbol{x}_{i,K} - \boldsymbol{x}_{c,K}|^2}} \quad \forall K \in \mathcal{T}_h, \tag{42}$$

where, for each element $K \in \mathcal{T}_h$, A_K is the area, $\boldsymbol{x}_{c,K}$ is the barycentre and $\boldsymbol{x}_{i,K}$, for $i = 1, 2, 3$, is the i-th vertex. The constant C_2 comes from the inverse inequality

$$\sum_{K \in \mathcal{T}_h} h_K^2 \int_K |\Delta v^{\mathcal{N}}|^2 \leq C_2 \|\nabla v^{\mathcal{N}}\|^2_{L^2(\Omega)} \quad \forall v^{\mathcal{N}} \in X^{\mathcal{N}} \subset \mathbb{P}^2(\mathcal{T}_h). \tag{43}$$

We refer to [8, 12] for the details.

In Table 2 we report some data about the tests we have performed, such as the Offline computational time, T_{off}, and the average effectivity of the *a posteriori* error estimator, $\eta^{av}_{N,stab}$, computed on a set Ξ_{test} with 100 elements. In each computation, the *truth* space dimension is $\mathcal{N} = 2605$.

r	$\mu_1 \in$	$\mu_2 \in$	$T_{\text{off}}\,(s)$	SCM iter	N	$\eta^{av}_{N,stab}$	$T_{\text{On}}(s)$
1	$\{10^4\}$	$[\frac{\pi}{6}, \frac{\pi}{3}]$	460	5	20	18.24	$1.74 \cdot 10^{-3}$
1	$\{10^5\}$	$[\frac{\pi}{6}, \frac{\pi}{3}]$	623	7	21	53.61	$1.75 \cdot 10^{-3}$
1	$[10^4, 10^5]$	$[\frac{\pi}{6}, \frac{\pi}{3}]$	688	8	36	75.48	$1.85 \cdot 10^{-3}$
1	$[10^4, 10^5]$	$\{\frac{\pi}{4}\}$	138	2	3	31.30	$1.49 \cdot 10^{-3}$
2	$\{10^4\}$	$[\frac{\pi}{6}, \frac{\pi}{3}]$	856	7	28	74.94	$1.94 \cdot 10^{-3}$
2	$\{10^5\}$	$[\frac{\pi}{6}, \frac{\pi}{3}]$	3856	19	29	172.44	$2.01 \cdot 10^{-3}$
2	$[10^4, 10^5]$	$[\frac{\pi}{6}, \frac{\pi}{3}]$	3067	28	66	154.63	$9.03 \cdot 10^{-3}$
2	$[10^4, 10^5]$	$\{\frac{\pi}{4}\}$	277	2	4	58.07	$1.74 \cdot 10^{-3}$

Table 2: Higher order polynomial approximation. Numerical tests

Remark 4.1. We observe that, when building the reduced basis, the variations of the advection field direction have more influence on the dimension N of the reduced basis than the variations of the Péclet number. Indeed, if we keep the advection field constant and we let vary only the Péclet number, the solution shows only variations of the "thickness" of the layers, whose position inside the domain does not change. On the contrary, if we let the advection field change, the position of the internal layer changes too. The reduced basis has then to be able to capture a parameter dependent layer and so, recalling that the reduced solution is a linear combination of the reduced basis functions, it is reasonable that the dimension N increases.

We note also that the Offline time is often much higher for the $\mathbb{P}^2$ approximation. This is because of the SCM, which needs more iterations in the $\mathbb{P}^2$ case than in the $\mathbb{P}^1$ one to provide stability factors approximations [15].

In Figure 14 we show some RB approximations obtained using a parameter space $\mathcal{D} = \{10^5\} \times [\frac{\pi}{6}, \frac{\pi}{3}]$. We note that the internal layer, whose position in the domain is parameter dependent, is well described in the RB solution.

5. Stabilized reduced basis method for time-dependent problems

In this section we want to extend our investigation to time dependent advection-diffusion equations. The RB method for time dependent problems has been already studied in several works, e.g. [9, 25, 28, 31], but, as regards the advection diffusion equations, we can only find applications with low Péclet number. In this work we are going to test a method that can be effectively applied to advection-diffusion problems with high Péclet number.

In Section 5.1 we introduce the general RB setting for parabolic problems, while in Section 5.2 we briefly recall the SUPG stabilization method for parabolic problems [2, 3, 19]. Finally, in Section 5.3, we show and discuss some numerical tests.

5.1. Reduced basis method for linear parabolic equations

As in Section 2.1, we define the *parameter domain* $\mathcal{D}$ as a closed subset of $\mathbb{R}^P$ and we call $\boldsymbol{\mu}$ any general P-tuple belonging to $\mathcal{D}$. Again, let Ω be a bounded open subset of $\mathbb{R}^d$ $(d = 1, 2, 3)$ with regular boundary $\partial\Omega$ and let X be a functional space such that $H^1_0(\Omega) \subset X \subset H^1(\Omega)$. For each admissible value of the parameter, i.e. for each $\boldsymbol{\mu} \in \mathcal{D}$, we define the continuous bilinear forms $a(\cdot, \cdot; \boldsymbol{\mu})\colon X \times X \to \mathbb{R}$ and $m(\cdot, \cdot; \boldsymbol{\mu})\colon L^2(\Omega) \times L^2(\Omega) \to \mathbb{R}$. We suppose that the form a satisfies the coercivity and *affinity* assumptions (2) and (4), respectively. We assume also that the *mass* form m satisfies a similar *affinity* assumption. Finally, for each $\boldsymbol{\mu} \in \mathcal{D}$, we define the right-hand side continuous linear form $F(\cdot; \boldsymbol{\mu})\colon X \to \mathbb{R}$ which satisfies the *affine* assumption (5).

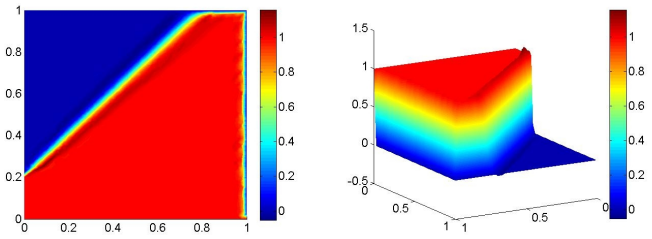

(a) $\mathbb{P}^1$-RB solution

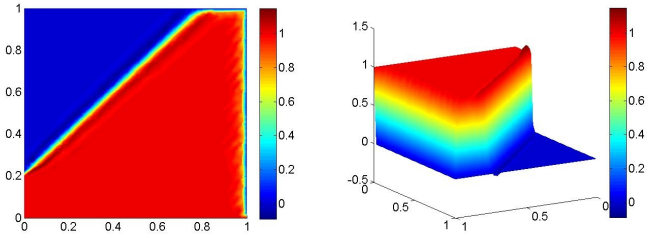

(b) $\mathbb{P}^2$-RB solution

Figure 14: $\mathbb{P}^1$-RB and $\mathbb{P}^2$-RB approximated solution of (38), with $\boldsymbol{\mu} = (10^5, \frac{\pi}{4})$.

Let us finally denote our time domain with $I = [0, T]$, where T is the final time. We can now define our continuous problem, as usually done in the RB framework [10, 25]:

$$\begin{aligned} &\text{find } u(\cdot;\boldsymbol{\mu}) \in C^0(I; L^2(\Omega)) \cap L^2(I; X) \text{ s.t.} \\ &m(\partial_t u(t;\boldsymbol{\mu}), v) + a(u(t;\boldsymbol{\mu}), v;\boldsymbol{\mu}) = g(t)F(v;\boldsymbol{\mu}) \quad \forall v \in X, \quad \forall t \in I \\ &\text{given the initial value } u(0;\boldsymbol{\mu}) = u_0 \in L^2(\Omega). \end{aligned} \tag{44}$$

where $g\colon I \to R$ is a *control function* such that $g \in L^2(I)$. We chose a right hand side of the form $g(t)F(v;\boldsymbol{\mu})$, as usual in the RB framework [10, 25], in order to ease the Offline-Online computational decoupling. In particular, the function g can be specified during the Online evaluation of the RB solution.

5.1.1. Discretization and RB formulation

To discretize the time-dependent problem (44) we follow the approach used in [10, 22, 25] which consists in using finite differences in time and FE in space discretization [27].

To obtain a fully discretized problem, we subdivide the time interval I into J subintervals of length $\Delta t = T/J$ and we define $t^j = j\Delta t$, $j = 1, \ldots, J$. The fully discretized problem we are considering is:

$$\begin{aligned} &\text{for each } 1 \le j \le J, \text{ find } u^{\mathcal{N}\,j}(\boldsymbol{\mu}) \in X^{\mathcal{N}} \text{ s.t.} \\ &\frac{1}{\Delta t} m(u^{\mathcal{N}\,j}(\boldsymbol{\mu}) - u^{\mathcal{N}\,j-1}(\boldsymbol{\mu}), v^{\mathcal{N}};\boldsymbol{\mu}) + a(u^{\mathcal{N}\,j}(\boldsymbol{\mu}), v^{\mathcal{N}};\boldsymbol{\mu}) = g(t^j)F(v^{\mathcal{N}};\boldsymbol{\mu}) \quad \forall v^{\mathcal{N}} \in X^{\mathcal{N}}, \\ &\text{given the initial condition } u^{\mathcal{N}\,0} \text{ s.t.} \\ &(u^{\mathcal{N}\,0}, v^{\mathcal{N}})_{L^2(\Omega)} = (u_0, v^{\mathcal{N}})_{L^2(\Omega)} \quad \forall v^{\mathcal{N}} \in X^{\mathcal{N}}. \end{aligned} \tag{45}$$

The latter problem is the *Backward Euler-Galerkin* approximation of (44). Of course, this is not the only way to discretize the time-dependent problem (44), for example we can resort to other theta-methods (e.g. Crank-Nicholson) or to higher order methods [27].

The RB formulation of the problem is based on a RB space whose basis functions are built by properly combining *snapshots* in time and space. More precisely, we construct the reduced basis in the time-dependent case following the so called *POD-Greedy* approach [11, 21, 22, 25]. It consists in using a Greedy technique to explore the parameter space $\mathcal{D}$ and the Proper Orthogonal Decomposition (POD) method to deal with the time evolution. For the *a posteriori* error estimates, we follow the choice presented in [10], but other possibilities have recently been proposed [32, 33]. The RB formulation of the problem can be obtained by substituting the reduced basis space $X_N^{\mathcal{N}}$ to $X^{\mathcal{N}}$ in (45).

5.2. SUPG stabilization method for time dependent problems

In this section we briefly introduce the SUPG method for time-dependent problems [2, 3, 19]. The idea is the same of the steady case: we add a stabilization term to the bilinear form in order to improve the stability. The stabilization term is almost the same than in the steady case, but now we have to consider also the time dependency to guarantee the strong consistency. We thus set

$$s(v^{\mathcal{N}}(t), w^{\mathcal{N}}; \boldsymbol{\mu}) = \sum_{K \in \mathcal{T}_h} \delta_K \left(\partial_t v^{\mathcal{N}}(t) + L^{\boldsymbol{\mu}} v^{\mathcal{N}}(t), \frac{h_K}{|\boldsymbol{\beta}(\boldsymbol{\mu})|} L^{\boldsymbol{\mu}}_{SS} w^{\mathcal{N}} \right)_K \tag{46}$$

where $v^{\mathcal{N}}(t) \in X^{\mathcal{N}}$ for each $t \in I$ and $w^{\mathcal{N}} \in X^{\mathcal{N}}$. Here $L^{\boldsymbol{\mu}}$ is the steady advection-diffusion operator and $L^{\boldsymbol{\mu}}_{SS}$ its skew-symmetric part (3).

We note that if either the coefficients of the equation or its domain are $\boldsymbol{\mu}$-dependent, then the stabilization terms will depend on $\boldsymbol{\mu}$ too, as we have actually shown in Section 3.

Assuming the parameter dependence, we can define the *Backward Euler-SUPG* formulation of the problem by substituting the forms m, a and F in (45) with

$$\begin{aligned}
m_{stab}(v^{\mathcal{N}}, w^{\mathcal{N}}; \boldsymbol{\mu}) &= m(v^{\mathcal{N}}, w^{\mathcal{N}}; \boldsymbol{\mu}) \; + \sum_{K_o(\boldsymbol{\mu}) \in \mathcal{T}_{h,o}(\boldsymbol{\mu})} \delta_{K_o(\boldsymbol{\mu})} \left(v^{\mathcal{N}}, \frac{h_{K_o(\boldsymbol{\mu})}}{|\boldsymbol{\beta}(\boldsymbol{\mu})|} L^{\boldsymbol{\mu}}_{SS}\, w^{\mathcal{N}} \right)_{K_o(\boldsymbol{\mu})} \\
a_{stab}(v^{\mathcal{N}}, w^{\mathcal{N}}; \boldsymbol{\mu}) &= a(v^{\mathcal{N}}, w^{\mathcal{N}}; \boldsymbol{\mu}) \; + \sum_{K_o(\boldsymbol{\mu}) \in \mathcal{T}_{h,o}(\boldsymbol{\mu})} \delta_{K_o(\boldsymbol{\mu})} \left(L^{\boldsymbol{\mu}} v^{\mathcal{N}}, \frac{h_{K_o(\boldsymbol{\mu})}}{|\boldsymbol{\beta}(\boldsymbol{\mu})|} L^{\boldsymbol{\mu}}_{SS}\, w^{\mathcal{N}} \right)_{K_o(\boldsymbol{\mu})} \\
F_{stab}(v^{\mathcal{N}}; \boldsymbol{\mu}) &= F(v^{\mathcal{N}}; \boldsymbol{\mu}) \; + \sum_{K_o(\boldsymbol{\mu}) \in \mathcal{T}_{h,o}(\boldsymbol{\mu})} \delta_{K_o(\boldsymbol{\mu})} \left(f, \frac{h_{K_o(\boldsymbol{\mu})}}{|\boldsymbol{\beta}(\boldsymbol{\mu})|} L^{\boldsymbol{\mu}}_{SS}\, w^{\mathcal{N}} \right)_{K_o(\boldsymbol{\mu})}
\end{aligned} \tag{47}$$

where $K_o(\boldsymbol{\mu})$ are the elements which form the mesh $\mathcal{T}_{h,o}$ defined on the original domain Ω_o and f can be a source term of the advection-diffusion equation or a lifting of the Dirichlet boundary data. For the analysis of stability and convergence of this method, we refer to [2, 4, 17].

5.3. Numerical results

We are showing now some numerical tests of the stabilized RB method for parabolic PDEs. The first one, discussed in Section 5.3.1 is the time dependent version of the problem studied in Section 4, while the second test case, Section 5.3.2, is a time-dependent Poiseuille-Graetz problem. In all our numerical test we considered $\mathbb{P}^1$ finite elements for the spatial discretization.

5.3.1. A first time dependent test case

Let us denote with Ω the unit square in $\mathbb{R}^2$, sketched in Figure 13. Moreover, let us denote with I the time interval $[0, T]$. Finally, let us define $\boldsymbol{\mu} = (\mu_1, \mu_2)$, with $\mu_1, \mu_2 \in \mathbb{R}$. The problem we are dealing with is the following:

$$\begin{cases}
\partial_t u - \dfrac{1}{\mu_1} \Delta u(\boldsymbol{\mu}) + (\cos\mu_2, \sin\mu_2) \cdot \nabla u(\boldsymbol{\mu}) = 0 & \text{in } \Omega \times I \\
u(\cdot, t; \boldsymbol{\mu}) = g(t) & \text{on } \Gamma_1 \cup \Gamma_2,\ \forall t \in I \\
u(\cdot, t; \boldsymbol{\mu}) = 0 & \text{on } \Gamma_3 \cup \Gamma_4 \cup \Gamma_5,\ \forall t \in I, \\
u(\cdot, 0; \boldsymbol{\mu}) = 0 & \text{on } \Omega,
\end{cases} \tag{48}$$

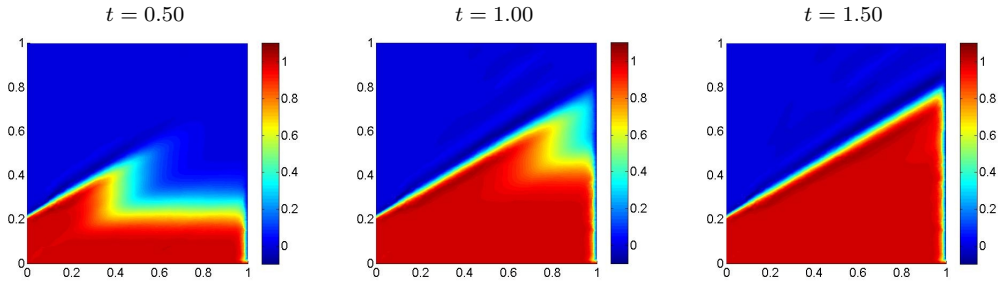

Figure 15: First time dependent test case. RB solution of (48), with $g(t) = 1$ for all $t \in [0, T]$, for a parameter value $\boldsymbol{\mu} = (10^5, \frac{\pi}{6})$.

where g is a control function.

The computations were performed using $T = 2.5$ and subdividing the time interval into $J = 50$ time-steps. As regards the spatial discretization, we used a mesh with size $h \approx 0.03$. The dimension of the polynomial approximation space is $\mathcal{N} = 2605$. The tolerance on the POD-Greedy algorithm is $\varepsilon^*_{tol} = 10^{-2}$ (see [25] for the definition). In Table 3 we report informations about the computational time and the average efficiency of the error estimator for the stabilized parabolic problem [25] (computed on a set Ξ_{test} with 100 elements). We note that the variations of the parameter μ_2, that is the direction of the advection field, has stronger effect on the number of reduced basis N than the variations of the Péclet number μ_1, as we observed also in the steady case in Section 4. In Figures 15 we report some pictures of the RB solutions obtained for $\boldsymbol{\mu} = (10^5, \frac{\pi}{6})$, using the parameter space $\mathcal{D} = [10^4, 10^5] \times [\frac{\pi}{6}, \frac{\pi}{3}]$. More precisely, in Figure 15, we show the RB solution (computed at some time-steps) of (48) obtained using a constant control function $g \equiv 1$.

$\mu_1 \in$	$\mu_2 \in$	$T_{\text{off}}\,(s)$	N	$T_{\text{on}}\,(s)$	$\eta^{av}_{N,stab}$
$\{10^5\}$	$[\frac{\pi}{6}, \frac{\pi}{3}]$	2346	28	$8.75 \cdot 10^{-2}$	2.35
$[10^4, 10^5]$	$[\frac{\pi}{6}, \frac{\pi}{3}]$	2857	69	$8.19 \cdot 10^{-2}$	3.43
$[10^4, 10^5]$	$\{\frac{\pi}{4}\}$	339	15	$8.44 \cdot 10^{-2}$	1.93

Table 3: First time dependent test case. Numerical tests

5.3.2. Time dependent Poiseuille-Graetz problem

In this section we want to test the stabilized RB method for a time dependent Poiseuille-Graetz problem [9, 16, 25, 31]. We have already dealt with the steady case of this problem in Section 3.2.

Let $\boldsymbol{\mu} = (\mu_1, \mu_2) \in \mathbb{R}^2$ such that $\mu_1, \mu_2 > 0$. For each value of the parameter $\boldsymbol{\mu}$, let $\Omega_o(\boldsymbol{\mu})$ be the rectangle in $\mathbb{R}^2$ sketched in Figure 7. We then define I the time interval $[0, T]$.

The problem is to find the temperature distribution $u(\boldsymbol{\mu})$ such that:

$$\begin{cases} \partial_t u(\boldsymbol{\mu}) - \dfrac{1}{\mu_1}\Delta u(\boldsymbol{\mu}) + 4\,y(1-y)\partial_x u(\boldsymbol{\mu}) = 0 & \text{in } \Omega_o(\boldsymbol{\mu}) \\ u(\cdot, t; \boldsymbol{\mu}) = g_1(t) & \text{on } \Gamma_{o\,1}(\boldsymbol{\mu}) \cup \Gamma_{o\,2}(\boldsymbol{\mu}) \cup \Gamma_{o\,6}(\boldsymbol{\mu}),\ \forall\, t \in I, \\ u(\cdot, t; \boldsymbol{\mu}) = g_2(t) & \text{on } \Gamma_{o\,3}(\boldsymbol{\mu}) \cup \Gamma_{o\,5}(\boldsymbol{\mu}),\ \forall\, t \in I, \\ \dfrac{\partial u}{\partial \nu}(\cdot, t; \boldsymbol{\mu}) = 0 & \text{on } \Gamma_{o\,4}(\boldsymbol{\mu}),\ \forall\, t \in I, \\ u(\cdot, 0; \boldsymbol{\mu}) = 1 & \text{on } \Omega_o(\boldsymbol{\mu}). \end{cases} \tag{49}$$

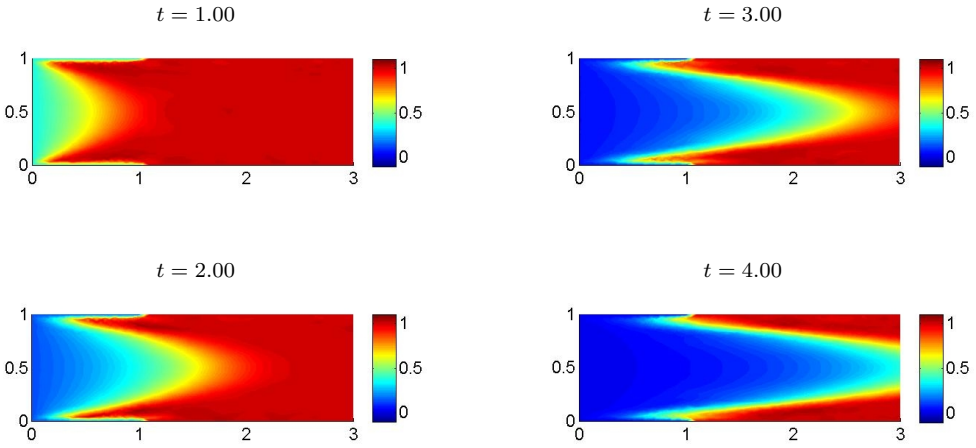

Figure 16: Time dependent Poiseuille-Graetz problem. RB solution computed at some time steps.

where g_1 and g_2 are *control* functions, which allow to impose time-dependent Dirichlet boundary conditions.

As problem (49) has Dirichlet boundary conditions depending on two different control functions, the right-hand side of the associated weak formulation will be of the form $g^1(t)F^1_{stab}(\cdot;\boldsymbol{\mu}) + g^2(t)F^2_{stab}(\cdot;\boldsymbol{\mu})$. The addends of the right-hand side are associated with the boundary conditions on $\Gamma_{o\,1}(\boldsymbol{\mu}) \cup \Gamma_{o\,2}(\boldsymbol{\mu}) \cup \Gamma_{o\,6}(\boldsymbol{\mu})$ and on $\Gamma_{o\,3}(\boldsymbol{\mu}) \cup \Gamma_{o\,5}(\boldsymbol{\mu})$, respectively. In order to effectively perform a reduced order approximation of problem (49), we decided to exploit the superposition of effects. We then considered two distinct subproblems, one for each term of the right hand side, whose solution is approximated with the RB method. The reduced solution of problem (49) is computed by summing the RB solutions of the two subproblems.

In our numerical tests we have used $\mathcal{D} = [10000, 20000] \times [0.5, 4]$, $T = 5$, $J = 100$ and $\theta = 1$. The dimension of the FE space is $\mathcal{N} = 1309$ ($h \approx 0.06$). The RB method yields $N^1 = 54$ basis for the problem with right-hand side $g^1(t)F^1_{stab}(\cdot;\boldsymbol{\mu})$ (Offline computational time: $1706\,s$) and $N^2 = 102$ basis for the problem with right-hand side $g^2(t)F^2_{stab}(\cdot;\boldsymbol{\mu})$ (Offline computational time: $6423\,s$). The tolerance on the Greedy algorithm is $\varepsilon^*_{tol} = 10^{-2}$ (see [25] for the definition).

In Figure 16, we show the RB solution of (49) for $\boldsymbol{\mu} = (15000, 2)$, computed at some time steps. Here we used as control functions: $g_1(t) = e^{-t}$ and $g_2(t) = 1$, for all $t \in I$. The computational time of the Online stage is $0.255\,s$. The average effectivity $\eta^{av}_{N,stab}$, computed on a set Ξ_{test} with 100 elements, is 1.85.

6. Conclusions

In this work we have dealt with stabilization techniques for the approximation of the solution of advection dominated problems using the reduced basis approach, in both steady and unsteady case, for high Péclet numbers.

Concerning the steady case, we have carried out a comparison between two possible stabilization techniques, an *Offline-Online* stabilization strategy and an *Offline-only* option. The *Offline-Online* strategy has turned out to be the best choice because it produces stable RB solutions and also the *a posteriori* error estimators discussed in [25, 29] are still effective. As regards the *Offline-only* method, we have observed strong instability phenomena in the RB solution and we have shown that this is because of "inconsistency" problems arising from the use of different bilinear forms in the

two stages of the RB method. We have provided also some explanations of the different behaviour of the two stabilization techniques based on physical considerations involving the advection field and the boundary layer.

We performed also some numerical test on a problem with steep boundary layers and an internal layer that strongly depend on the direction of the parametric advection field.

In the last part of our work, we have developed a stabilization strategy for the RB approximation of time dependent advection dominated problems. The FE stabilization method - on which our strategy has been based upon - is a time-dependent SUPG method [2, 3]. Considering what we have shown in the steady case, we have proposed to use the same stabilized form in both Offline and Online stage. The method has been successfully tested on some test problems, in particular on an unsteady Poiseuille-Graetz problem with time dependent boundary conditions.

Possible further developments will be related to stabilization techniques for nonlinear problems, e.g. Navier-Stokes equations to increase Reynolds number.

7. Acknowledgements

P. Pacciarini acknowledges the support provided by the Erasmus Student Placement Project of the University of Pavia, Italy, to allow a research period at École Polytechnique Fédérale de Lausanne, Switzerland, Mathematics Institute of Computational Science and Engineering.

G. Rozza acknowledges the program NOFYSAS, New Opportunities for Young Scientists at SISSA, International School for Advanced Studies, Trieste, Italy.

Both authors wish to thank Prof. Ilaria Perugia, University of Pavia, for her helpful contributions to this work.

The computations in this work have been performed in MATLAB® software using the MLife (finite elements) library and an enhanced version (co-developed at CMCS, EPFL) of the rbMIT© library [14, 23]. These libraries have been extended while carrying out this work, implementing the stabilization methods studied and used.

[1] M. Barrault, Y. Maday, N.C. Nguyen, and A.T. Patera. An 'empirical interpolation' method: application to efficient reduced-basis discretization of partial differential equations. *C. R. Math. Acad. Sci. Paris*, 339(9):667–672, 2004.

[2] P.B. Bochev, M.D. Gunzburger, and J.N. Shadid. Stability of the SUPG finite element method for transient advection-diffusion problems. *Comput. Methods Appl. Mech. Engrg.*, 193(23-26):2301–2323, 2004.

[3] A.N. Brooks and T.J.R. Hughes. Streamline upwind/Petrov-Galerkin formulations for convection dominated flows with particular emphasis on the incompressible Navier-Stokes equations. *Comput. Methods Appl. Mech. Engrg.*, 32(1-3):199–259, 1982. FENOMECH '81, Part I (Stuttgart, 1981).

[4] E. Burman and G. Smith. Analysis of the space semi-discretized SUPG method for transient convection-diffusion equations. *Math. Models Methods Appl. Sci.*, 21(10):2049–2068, 2011.

[5] W. Dahmen, C. Plesken, and G. Welper. Double greedy algorithms: reduced basis methods for transport dominated problems. 2013. Submitted.

[6] L. Dedè. *Adaptive and reduced basis approach for optimal control problems in environmental applications*. PhD thesis, Politecnico di Milano, 2008.

[7] L. Dedè. Reduced basis method for parametrized elliptic advection-reaction problems. *J. Comput. Math.*, 28(1):122–148, 2010.

[8] L.P. Franca, S.L. Frey, and T.J.R. Hughes. Stabilized finite element methods. I. Application to the advective-diffusive model. *Comput. Methods Appl. Mech. Engrg.*, 95(2):253–276, 1992.

[9] F. Gelsomino and G. Rozza. Comparison and combination of reduced-order modelling techniques in 3D parametrized heat transfer problems. *Math. Comput. Model. Dyn. Syst.*, 17(4):371–394, 2011.

[10] M.A. Grepl and A.T. Patera. A posteriori error bounds for reduced-basis approximations of parametrized parabolic partial differential equations. *M2AN Math. Model. Numer. Anal.*, 39(1):157–181, 2005.

[11] B. Haasdonk and M. Ohlberger. Reduced basis method for finite volume approximations of parametrized linear evolution equations. *M2AN Math. Model. Numer. Anal.*, 42(2):277–302, 2008.

[12] I. Harari and T.J.R. Hughes. What are C and h?: inequalities for the analysis and design of finite element methods. *Comput. Methods Appl. Mech. Engrg.*, 97(2):157–192, 1992.

[13] T.J.R. Hughes and A. Brooks. A multidimensional upwind scheme with no crosswind diffusion. In *Finite element methods for convection dominated flows*, volume 34 of *AMD*, pages 19–35. Amer. Soc. Mech. Engrs. (ASME), New York, 1979.

[14] D.B.P. Huynh, N.C. Nguyen, A.T. Patera, and G. Rozza. Rapid reliable solution of the parametrized partial differential equations of continuum mechanics and transport. Available at `http://augustine.mit.edu`. Copyright MIT 2008-2011.

[15] D.B.P. Huynh, G. Rozza, S. Sen, and A.T. Patera. A successive constraint linear optimization method for lower bounds of parametric coercivity and inf-sup stability constants. *C. R. Math. Acad. Sci. Paris*, 345(8):473–478, 2007.

[16] F.P. Incropera and D.P. DeWitt. *Fundamentals of Heat and Mass Transfer*. John Wiley & Sons, 1990.

[17] V. John and J. Novo. Error analysis of the SUPG finite element discretization of evolutionary convection-diffusion-reaction equations. *SIAM J. Numer. Anal.*, 49(3):1149–1176, 2011.

[18] C. Johnson and U. Nävert. An analysis of some finite element methods for advection-diffusion problems. In *Analytical and numerical approaches to asymptotic problems in analysis (Proc. Conf., Univ. Nijmegen, Nijmegen, 1980)*, volume 47 of *North-Holland Math. Stud.*, pages 99–116. North-Holland, Amsterdam, 1981.

[19] C. Johnson, U. Nävert, and J. Pitkäranta. Finite element methods for linear hyperbolic problems. *Comput. Methods Appl. Mech. Engrg.*, 45(1-3):285–312, 1984.

[20] F. Negri, G. Rozza, A. Manzoni, and A. Quarteroni. Reduced basis method for parametrized elliptic optimal control problems. To appear in SIAM Journal on Scientific Computing, 2013.

[21] N. C. Nguyen, G. Rozza, and A. T. Patera. Reduced basis approximation and a posteriori error estimation for the time-dependent viscous Burgers' equation. *Calcolo*, 46:157–185, 2009.

[22] N.C. Nguyen, G. Rozza, D.B.P. Huynh, and A.T. Patera. Reduced basis approximation and a posteriori error estimation for parametrized parabolic PDEs: application to real-time Bayesian parameter estimation. In *Large-scale inverse problems and quantification of uncertainty*, Wiley Ser. Comput. Stat., pages 151–177. Wiley, Chichester, 2010.

[23] A.T. Patera and G. Rozza. *Reduced Basis Approximation and A Posteriori Error Estimation for Parametrized Partial Differential Equations*. Version 1.0, Copyright MIT 2006-2007, to appear in (tentative rubric) MIT Pappalardo Graduate Monographs in Mechanical Engineering. Available at `http://augustine.mit.edu`.

[24] A. Quarteroni, G. Rozza, L. Dedè, and A. Quaini. Numerical approximation of a control problem for advection-diffusion processes. In *System modeling and optimization*, volume 199 of *IFIP Int. Fed. Inf. Process.*, pages 261–273. Springer, New York, 2006.

[25] A. Quarteroni, G. Rozza, and A. Manzoni. Certified reduced basis approximation for parametrized partial differential equations and applications. *J. Math. Ind.*, 1:1(3), 2011.

[26] A. Quarteroni, G. Rozza, and A. Quaini. Reduced basis methods for optimal control of advection-diffusion problem. In W. Fitzgibbon, R. Hoppe, J. Periaux, O. Pironneau, and Y. Vassilevski, editors, *Advances in Numerical Mathematics*, pages 193–216, Moscow, Russia and Houston, USA, 2007.

[27] A. Quarteroni and A. Valli. *Numerical Approximation of Partial Differential Equations*, volume 23 of *Springer Series in Computational Mathematics*. Springer-Verlag, Berlin, 1994.

[28] G. Rozza, D.B.P. Huynh, N.C. Nguyen, and A.T. Patera. Real-time reliable simulation of heat transfer phenomena. In *ASME -American Society of Mechanical Engineers - Heat Transfer Summer Conference Proceedings, HT2009 3 , pages 851-860*, S. Francisco, CA, USA, 2009.

[29] G. Rozza, D.B.P. Huynh, and A.T. Patera. Reduced basis approximation and a posteriori error estimation for affinely parametrized elliptic coercive partial differential equations: application to transport and continuum mechanics. *Arch. Comput. Methods Eng.*, 15(3):229–275, 2008.

[30] G. Rozza, T. Lassila, and A. Manzoni. Reduced basis approximation for shape optimization in thermal flows with a parametrized polynomial geometric map. In J.S. Hesthaven and E. M. RRønquist, editors, *Spectral and High Order Methods for Partial Differential Equations*, volume 76 of *Lecture Notes in Computational Science and Engineering*, pages 307–315. Springer Berlin Heidelberg, 2011.

[31] G. Rozza, N.C. Nguyen, A.T. Patera, and S. Deparis. Reduced basis methods and a posteriori error estimators for heat transfer problems. In *ASME -American Society of Mechanical Engineers - Heat Transfer Summer Conference Proceedings, HT2009 2 , pages 753-762*, S. Francisco, CA, USA, 2009.

[32] K. Urban and A.T. Patera. An improved error bound for reduced basis approximation of linear parabolic problems. To appear in Mathematics of Computation.

[33] K. Urban and A.T. Patera. A new error bound for reduced basis approximation of parabolic partial differential equations. *C. R. Math. Acad. Sci. Paris*, 350(3-4):203–207, 2012.

Recent publications :

MATHEMATICS INSTITUTE OF COMPUTATIONAL SCIENCE AND ENGINEERING
Section of Mathematics
Ecole Polytechnique Fédérale
CH-1015 Lausanne

31.2013 R. GRANAT, B. KAGSTRÖM, D. KRESSNER, M. SHAO:
Parallel library software for the multishift QR algorithm with aggressive early deflation

32.2013 P. CHEN, A. QUARTERONI:
Weighted reduced basis method for stochastic optimal control problems with elliptic PDE contstraint

33.2013 P. CHEN, A. QUARTERONI, G. ROZZA:
Multilevel and weighted reduced basis method for stochastic optimal control problems constrained by Stokes equations

34.2013 A. ABDULLE, M. J. GROTE, C. STOHRER:
Finite element heterogeneous multiscale method for the wave equation: long time effects

35.2013 A. CHKIFA, A. COHEN, G. MIGLIORATI, F. NOBILE, R. TEMPONE:
Discreate least squares polynomial approximation with random evaluations-application to parametric and stochastic elliptic PDEs

36.2013 N. GUGLIELMI, D. KRESSNER, C. LUBICH:
Computing extremal points of symplectic pseudospectra and solving symplectic matrix nearness problems

37.2013 S. DEPARIS, D. FORTI, A. QUARTERONI:
A rescaled localized radial basis functions interpolation on non-cartesian and non-conforming grids

38.2013 A. GIZZI, R. RUIZ-BAIER, S. ROSSI, A. LAADHARI, C. CHERUBINI, S. FILIPPI:
A three-dimensional continuum model of active contraction in single cardiomyocytes

39.2013 P. TRICERRI, L. DEDÈ, A. QUARTERONI, A. SEQUEIRA:
Numerical validation of isotropic and transversely isotropic constitutive models for healthy and unhealthy cerebral arterial tissues

40.2013 D. KRESSNER, M. STEINLECHNER, A. USCHMAJEW:
Low-rank tensor methods with subspace correction for symmetric eigenvalue problems

41.2013 A. ABDULLE, O. BUDÁC:
An adaptive finite element heterogeneous multiscale method for Stokes flow in porous media

42.2013 C. JÄGGLI, L.IAPICHINO, G. ROZZA:
An improvement on geometrical parametrizations by transfinite maps

43.2013 P. PACCIARINI, G. ROZZA:
Stabilized reduced basis method for parametrized advection-diffusion PDEs